Research article

LUMINESCENCE
The Journal of Biological and Chemical Luminescence

Received: 12 July 2015, Revised: 24 August 2015, Accepted: 2 September 2015 Published online in Wiley Online Library: 15 October 2015

(wileyonlinelibrary.com) DOI 10.1002/bio.3043

Sensitive detection of strong acidic condition by a novel rhodamine-based fluorescent pH chemosensor

Jia-Lian Tan,[a] Ting-Ting Yang,[a] Yu Liu,[a] Xue Zhang,[a] Shu-Jin Cheng,[a] Hua Zuo[a]* and Huawei He[b]*

ABSTRACT: A novel rhodamine-based fluorescent pH probe responding to extremely low pH values has been synthesized and characterized. This probe showed an excellent photophysical response to pH on the basis that the colorless spirocyclic structure under basic conditions opened to a colored and highly fluorescent form under extreme acidity. The quantitative relationship between fluorescence intensity and pH value (1.75–2.62) was consistent with the equilibrium equation $pH = pKa + \log[(I_{max} - I)/(I - I_{min})]$. This sensitive pH probe was also characterized with good reversibility and no interaction with interfering metal ions, and was successfully applied to image *Escherichia coli* under strong acidity. Copyright © 2015 John Wiley & Sons, Ltd.

Additional supporting information may be found in the online version of this article at the publisher's web site.

Keywords: extreme acidity; rhodamine-derived probe; pH; *E. coli*

Introduction

Intracellular pH plays an essential and sophisticated role in many cellular events, such as cellular metabolism (1,2), proliferation (3), signal transduction (4), chemotaxis (5), apoptosis (6) and autophagy (7). Monitoring pH changes inside living cells, therefore, contributes to exploring cellular functions and understanding physiological and pathological processes in organisms.

Among the developed methods for measuring the intracellular pH like microelectrodes, nuclear magnetic resonance (NMR), absorbance spectroscopy and fluorescence spectroscopy, fluorescence techniques have attracted the most attention due to their high selectivity and sensitivity. We have noticed that some fluorescent pH probes were developed and even commercially available, such as green fluorescent protein and micromolecular pH sensors (8) derived from benzoxanthenes, cyanine (9), fluorescein (10) and others (11,12). However, these fluorescent pH sensors are only applicable to aqueous solutions in the pH range 4–9 (13–18) and it remains challenging to detect the very low intracellular pH. Challenges to develop fluorescent sensors that respond to extreme acidity are ascribed to the weak fluorescence and chemical instability of fluorescein or coumarin under strongly acidic conditions, the loss of selectivity due to the coordination with interfering metal ions of those reported pH-sensitive fluorescent probes containing carboxyl or hydroxyl functional groups and the lack of linear relationship between fluorescence intensity and pH due to the incorporation of too many receptors (19). In spite of the fact that most living species could hardly survive in extremely acidic environments, certain microorganisms, such as *Helicobacter pylori* and 'acidophiles' favor such harsh conditions (20–22). The stomach, the strongly acidic organ of mammals, even contains gastric juices with acidity pH 1.5–3.0, thereby activating digestive enzymes and also protecting the body from ingested microorganisms (20). The dilemma of the detection of precise pH values in the cellular compartments above prompts the development of novel fluorescent probes that can be applied to accurately monitor the acidic pH values in microorganisms.

Rhodamine derivatives have been widely used as 'turn-on' fluorescence probes (23–28) due to their unparalleled photophysical properties, such as high quantum yields, relatively long absorption and emission wavelengths in the visible region, large extinction coefficients and great photostability. The spirocyclic structure in rhodamine derivatives plays a major role in the response to the change of solvent pH value. It remains the spirocyclic form that is non-fluorescent and colorless at high pH (pH ≥7.0), while the ring-opened form exhibits strong fluorescence and a pink color at very low pH (29). Given that rhodamine derivatives are used to measure acidic pH values, we designed and synthesized a novel fluorescent pH-sensitive probe **L** constructed from rhodamine hydrazine, carbonylethylene and 1-phenylpiperazine, this

* Correspondence to: H. Zuo, College of Pharmaceutical Sciences, Southwest University, Chongqing 400715, China.
E-mail: zuohua@swu.edu.cn
* H. He, State Key Laboratory of Silkworm Genome Biology, Southwest University, Chongqing 400715, China.

[a] College of Pharmaceutical Sciences, Southwest University, Chongqing 400715, China

[b] State Key Laboratory of Silkworm Genome Biology, Southwest University, Chongqing 400715, China

Abbreviations: ICT, intramolecular charge transfer; MS, mass spectra; NMR, nuclear magnetic resonance; TLC, thin-layer chromatography.

probe exhibited much higher fluorescent intensity and quantum yield than that of certain probes working under strong acidic conditions (6,30–33). Compared with the sensor reported by our group (34), the probe is less prone to being interfered by coexisting metal ions due to the removal of the fluorine atom from the phenylpiperazinyl moiety.

Experimental

Materials

Deionized water was used throughout the experiments. All reagents were purchased from commercial suppliers and used without further purification. All samples were prepared at room temperature. Solvents were dried and purified by known conventional methods. The solutions of metal ions were prepared from nitrate salts, which were dissolved in deionized water. Britton-Robinson (B-R) buffer was a mixture of 40 mM acetic acid, boric acid and phosphoric acid. Dilute hydrochloric acid or sodium hydroxide was used for tuning pH values.

Instruments

Melting point (uncorrected) was determined on a micromelting point apparatus (Shanghai Shenguang Instrument Co., Ltd., China). ^{1}H and ^{13}C NMR spectra (at 400 MHz and 100 MHz, respectively) were recorded in $CDCl_3$ with tetramethylsilane as internal reference on a Bruker Advance 500 FT spectrometer. Chemical shifts were reported in parts per million. Mass spectra (MS) were measured by the electrospray ionization (ESI) method on an Agilent 6510 Q-TOF mass spectrometer. $CDCl_3$ delivered from Adamas Co., Ltd. (Shanghai, China) was used. Aluminium oxide (100–200 mesh) was used for flash column chromatography. All reactions were monitored by thin-layer chromatography (TLC) using 0.25 mm silica gel plates with an ultraviolet (UV) light indicator (Shanghai Jiapeng Technology Co., Ltd., China). UV–vis spectra were recorded on a UV-2550 spectrometry (Hitachi, Japan). Fluorescence was measured on a F-4500 FL spectrophotometer (Hitachi, Japan). The pH measurements were performed on a PHS-3C digital pH meter (Mettler Toledo, Switzerland). Images of *E. coli* cells were captured with a laser confocal microscope (Carl Zeiss LSM-700, Germany).

Synthesis of probe L

The synthetic route of probe **L** is outlined in Scheme 1. Chloroacetyl chloride (9.50 mmol, 2.0 equiv) was added dropwise to the solution of rhodamine hydrazide **2** (4.75 mmol, 1.0 equiv) (35) in 70 mL dichloromethane and the reaction mixture was then stirred for 10 h at room temperature, and excess triethylamine (47.50 mmol, 10.0 equiv) was added slowly into the solution. After completion of the reaction as indicated by TLC, the solvent was evaporated and the obtained solid was washed by 30 mL deionized water, dried and purified by column chromatography (elute: ethyl acetate:petroleum = 1:6 (v/v) to give the intermediate **3**. The solution of compound **3** (0.43 mmol, 1.0 equiv) and 1-phenylpiperazine (0.99 mmol, 0.7 equiv) was then heated in refluxing acetonitrile (18 mL) and generated the desired product in the presence of potassium carbonate (2.3 mmol, 2.0 equiv). The recrystallization from acetonitrile (20 mL) afforded probe **L** as white solid in 82.1% yield. m.p. 214.0–216.0 °C.

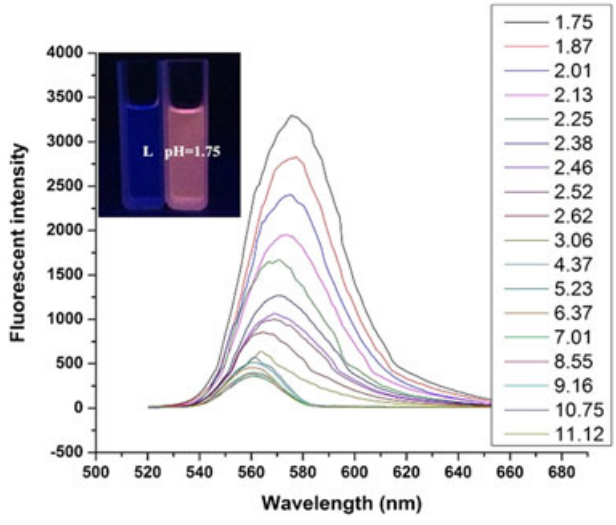

Figure 1. The fluorescence spectrum of **L** (25 μM) in solution (buffer:EtOH, v/v = 1:1) at different pH, λ_{ex} = 561 nm.

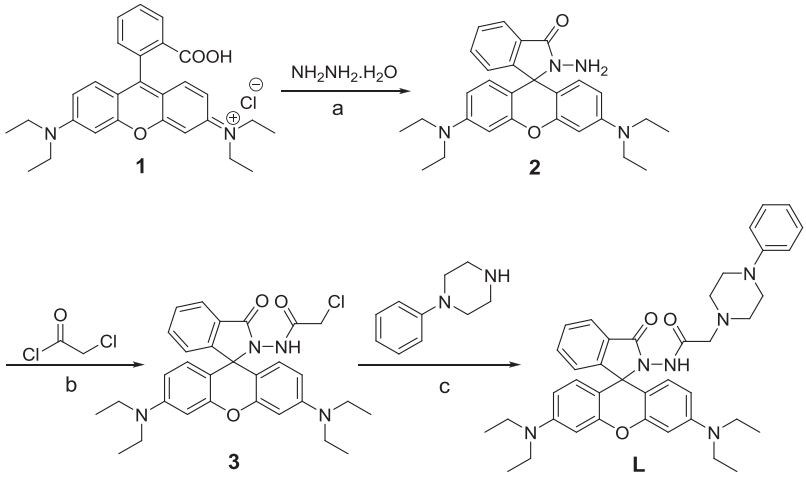

Scheme 1. The synthetic route for probe **L**. Reagents and conditions: (a) ethanol, reflux, 24 h; (b) Et_3N, CH_2Cl_2, r.t., 24 h; (c) K_2CO_3, CH_3CN, reflux, 3 h.

LUMINESCENCE
The Journal of Biological and Chemical Luminescence

Bacteria culture and imaging

E. coli cells were cultured at 37 °C in Luria-Bertani culture (tryptone 10 g/L, yeast extract 5 g/L, NaCl 10 g/L) in a table concentrator (AO HUA, ZD-85, China) shaking for 5 h at 180 rpm. The culture was then centrifuged (Heal Force TGL-16 M, China) at 10 000 rpm for 5 min and the obtained sediment was resuspended with B-R buffer at pH 1.75, 2.30 or 4.83, respectively. The probe dissolved in ethanol was then added into each buffer, at a final probe concentration of 25 μM after resuspension. The *E. coli* cells were incubated with the probe for 1 h, washed with deionized water and smeared onto slides. The obvious color change in *E. coli* cells was captured at 555 nm wavelength under laser confocal microscopy (Carl Zeiss lsm-700, Germany).

Results and discussion

Synthesis of probe L

Scheme 1 illustrates the general synthetic route for probe **L**. Firstly, rhodamine B (**1**) was reacted with hydrazine hydrate and cyclized to form the five-member ring in rhodamine hydrazide **2**, which then nucleophilically attacked the electron-deficient carbonyl of chloroacetyl chloride. The obtained amide **3** underwent *N*-alkylation with 1-phenylpiperazine to afford the probe **L**, which was characterized by ^{1}H NMR, ^{13}C NMR (Fig. S3, Fig. S4, Fig. S5) and HRMS. ^{1}H NMR (400 MHz, $CDCl_3$) δ 8.38 (s, 1H), 7.97 (d, *J* = 6.4 Hz, 1H), 7.54–7.46 (m, 2H), 7.23 (d, *J* = 8.0 Hz, 2H), 7.13 (d, *J* = 6.5 Hz, 1H), 6.88–6.83 (m, 3H), 6.65 (d, *J* = 8.7 Hz, 2H), 6.33–6.28 (m, 4H), 3.30–3.24 (m, 8H), 3.04 (s, 2H), 2.92 (s, 4H), 2.51–2.44 (m, 4H), 1.08 (t, *J* = 7.0 Hz, 12H). ^{13}C NMR (101 MHz, $CDCl_3$) δ 167.5, 165.3, 153.6, 151.5, 151.3, 149.0, 133.2, 129.5, 129.4, 129.0, 128.4, 124.1, 123.5, 120.0, 116.3, 108.2, 104.1, 97.4, 66.1, 60.4, 53.2, 49.5, 44.3, 31.0, 12.6. ESI-HRMS m/z: calcd for $[M+H]^+$ $C_{40}H_{47}N_6O_3^+$: 659.3710, found: 659.3713.

Spectroscopic properties and optical responses to pH

It was observed that the fluorescence intensity increased dramatically when the pH value of the buffer was decreasing from 3.06 to 1.75, in marked contrast to the slight increase of fluorescence intensity in the buffer ranging from basic to weakly acidic condition (Fig. 1). Simultaneously, the obvious pink color appeared under highly acidic condition, which was consistent with the proposed ring-opening mechanism of the probe. Specifically, the alkyl nitrogen atom of the piperazine was protonated upon the addition of trifluoroacetic acid and with the further protonation of the amide nitrogen atom in the spirolactam ring, the spirolactam ring subsequently opened to form a conjugated xanthene ring (Scheme 2), which was similar to the reported ring-opening process (36–39) .

The fluorescence intensity also showed a linear response to pH values between 1.75 and 2.62 with the function Y = −3008.96 pH + 8442.80 and R^2 = 0.9909, as shown in Fig. 2. This function further allowed us to calculate the pH value of any sample with pH ranged from 1.75 to 2.62. Therefore, probe **L** could be used as a highly sensitively colorimetric and fluorescent pH indicator.

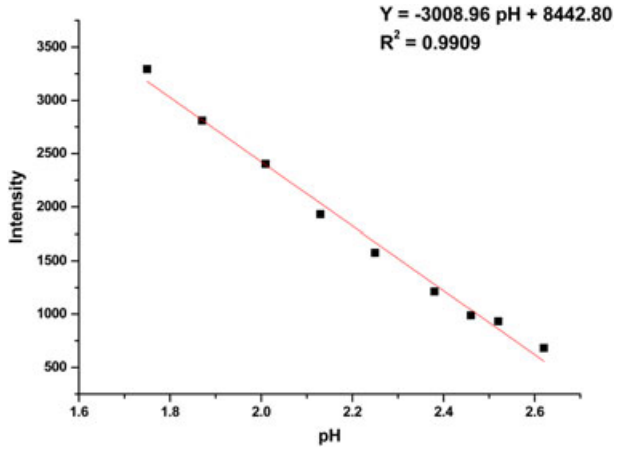

Figure 2. Linear regression based Intensity versus pH value. Equation: Y = −3008.96 pH + 8442.80, R^2 = 0.9909 (The data are the same with those in Fig. 1).

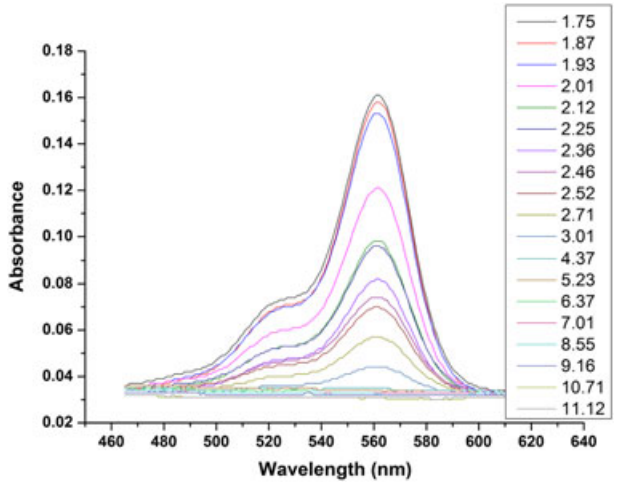

Figure 3. Absorption spectra of **L** (25 μM) in solution (buffer:EtOH, v/v = 1:1) with different pH.

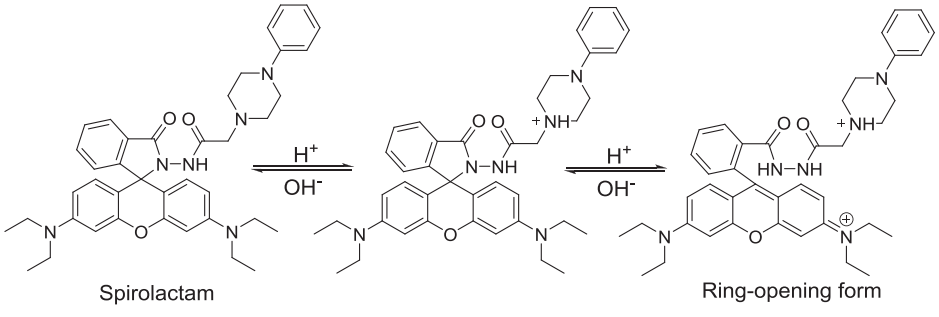

Scheme 2. Proposed ring-opening mechanism of probe **L**.

As illustrated in Fig. 3, the UV–vis absorption intensity increased upon the acidification of the neutral solution of probe **L**, especially under extremely acidic conditions (from pH 3.01 to 1.75), in agreement with the trend in fluorescence intensity. When the pH value varied from 3.01 to 1.75, both the absorbance at 560 nm and the fluorescence intensity at 575 nm were remarkably increased. However, the more significant increasing tendency in the fluorescence spectra than in the absorption spectra permitted us to efficiently evaluate pH values through fluorescence spectra.

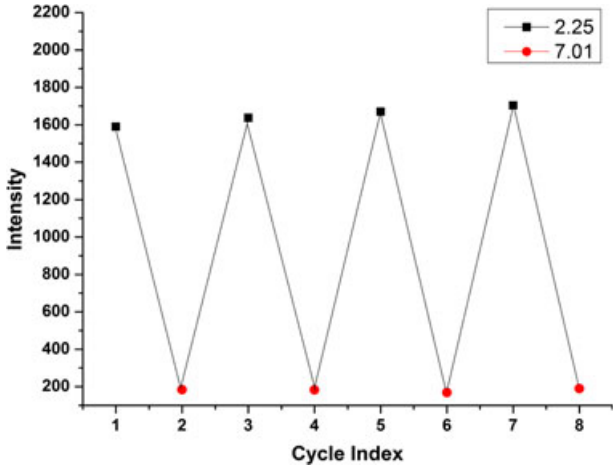

Figure 4. The fluorescence intensity at 575 nm of probe **L** (25 μM) between pH 2.25 and 7.15 in B-R buffer (excitation wavelength: 561 nm).

To investigate the reversibility of the fluorescence intensity versus pH, we changed the pH value of the buffer for the probe **L** from 2.25 to 7.15 by slowly adding NaOH solution and reversely acidifying the solution from 7.15 to 2.25 through HCl solution. The corresponding fluorescence intensity was detected and depicted in Fig. 4. The fluorescence intensity decreased dramatically from about 1600 to less than 250 with the neutralization of the strongly acidic buffer, accompanied by the disappearance of the noticeable pink color, which resulted from the conversion from the spirolactam form existing predominantly in neutral buffered media to the ring-opened amide structure upon the acidification of the solution. Despite the reversible changes of pH value between 2.25 and 7.15, the figures for fluorescence intensity remained nearly the same level at the same pH.

The probe **L** responded to extreme acidity quickly (less than 1 min) as illustrated by the time course of fluorescence intensity (Fig. S1). Since various metal ions, including Zn^{2+}, Ni^{2+}, Na^{+}, Mn^{2+}, Mg^{2+}, Li^{+}, K^{+}, Hg^{2+}, Fe^{3+}, Cu^{2+}, Ba^{2+}, Cs^{+}, Al^{3+}, Ag^{+}, Co^{2+}, or Ca^{2+} could not coordinate with the probe, they proved not to affect the pH-sensing properties of **L** (Fig. S2), which guaranteed the successful application of the probe **L** in complex ionized solutions.

pH bioimaging in live *E. coli*

The images of *E. coli* cells were captured by scanning confocal microscopy to investigate the ability of the probe to monitor pH value inside living cells. To simulate the extremely acidic

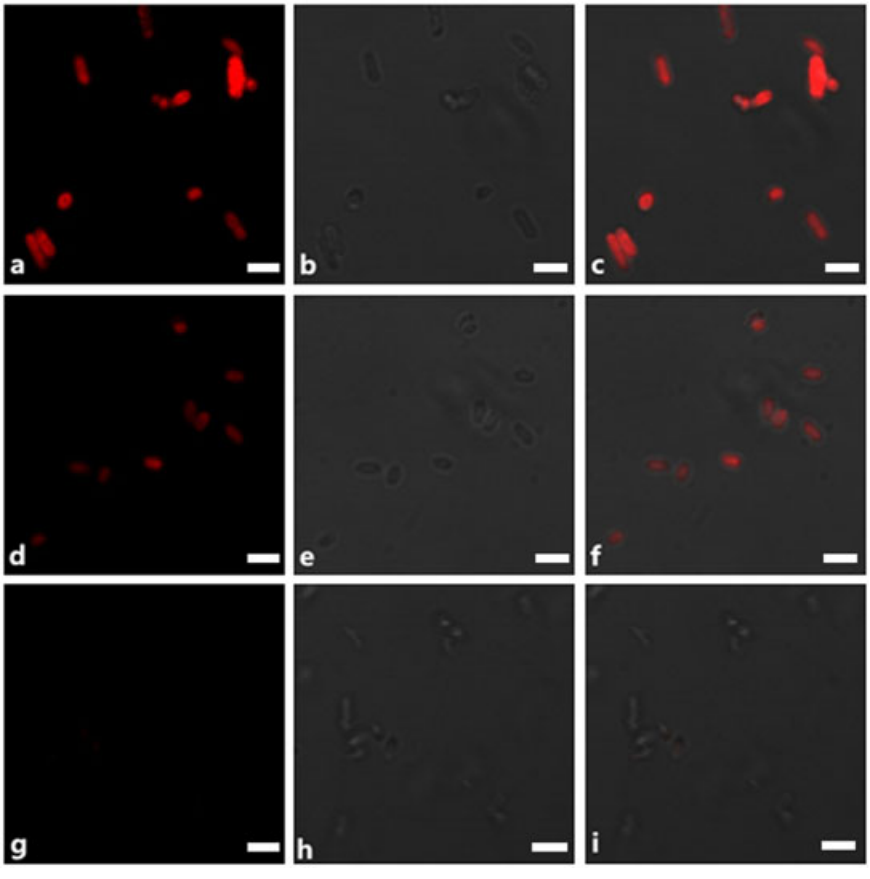

Figure 5. Imaging acidity in *E. coli* cells with probe **L**. (a–c) pH = 1.75; (d–f) pH = 2.30; (g–i) pH = 4.83. (a, d, g) are the fluorescence images; (b, e, h) are bright field images; (c, f, i) are merged images (scale bar: 5 μm).

LUMINESCENCE
The Journal of Biological and Chemical Luminescence

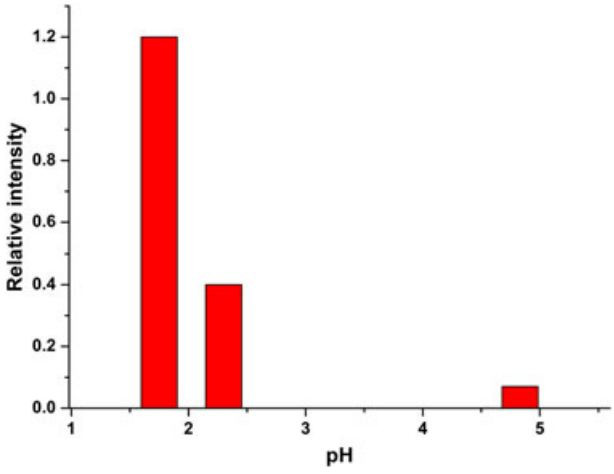

Figure 6. Quantitative analysis of fluorescence intensity in *E. coli* cells.

environment, the bacteria were incubated with acidic buffers at pH 1.75, 2.3 or 4.83, respectively. Red fluorescence was clearly observed in the bacteria due to the excellent cell membrane permeability and the fluorescence intensity inside *E. coli* cells increased dramatically with the increase in buffer acidity from pH 4.83 to pH 1.75 (Fig. 5). The quantitative analysis of the fluorescent intensity through ImageJ software followed the same trend (Fig. 6), which is in accordance with that of the fluorescence spectra. Direct and real-time monitoring of variations at extremely low pH in live biological systems is thus realized.

Conclusions

In summary, we have developed a novel fluorescent pH probe **L** based on rhodamine B with excellent selectivity and sensitivity to extremely acidic conditions. Apart from the strong selectivity due to no interference with the coexisted metal ions, good reversibility and short response time (<1 min) are also valuable characters of the probe. The fluorescence imaging of bacteria *E. coli* by the probe contributed to the development of more useful colorimetric and fluorescent sensors based on the rhodamine platform for measuring intracellular pH under extremely acidic conditions.

Acknowledgements

We would like to thank the Technology and Program Project of the Science and Technology Department of Sichuan Province (2015FZ0070) and the Fundamental Research Funds for the Central Universities (SWU112111, XDJK2013A019) for financial support.

References

1. Montgomery MT, Boyd TJ, Osburn CL, Plummer RE, Masutani SM, Coffin RB. Desalination technology waste streams: Effect of pH and salinity on metabolism of marine microbial assemblages. Desalination 2009;249:861–4.
2. Otomo T, Higaki K, Nanba E, Ozono K, Sakai N. Lysosomal storage causes cellular dysfunction in mucolipidosis II skin fibroblasts. J Biol Chem 2011;286:35283–90.
3. Bao YY, Keersmaecker HD, Corneillie S, Yu F, Mizuno H, Zhang GF, Hofkens J, Mendrek B, Kowalczuk A, Smet M. Tunable ratiometric fluorescence sensing of intracellular pH by aggregation-induced emission-active hyperbranched polymer nanoparticles. Chem Mater 2015;27:3450–5.
4. Sjöholm J, Havelius KGV, Mamedov F, Styring S. Effects of pH on the S_3 state of the oxygen evolving complex in photosystem II probed by EPR split signal induction. Biochemistry 2010;49:9800–8.
5. Zhang WS, Tang B, Liu X, Liu YY, Xu KH, Ma JP, Tong LL, Yang GW. A highly sensitive acidic pH fluorescent probe and its application to HepG2 cells. Analyst 2009;134:367–71.
6. Wiktorowski S, Daltrozzo E, Zumbusch A. Water-soluble pyrrolopyrrole cyanine (PPCy) near infrared fluorescent pH indicators for strong acidity. RSC Adv 2015;5:29420–3.
7. Wojtkowiak JW, Gillies RJ. Autophagy on acid. Autophagy 2012;8:1688–9.
8. Han JY, Burgess K. Fluorescent indicators for intracellular pH. Chem Rev 2010;110:2709–28.
9. Li YH, Wang YJ, Yang S, Zhao YR, Yuan L, Zheng J, Yang RH. Hemicyanine-based high resolution ratiometric near-infrared fluorescent probe for monitoring pH changes *in vivo*. Anal Chem 2015;87:2495–503.
10. Qian ZQ, Dougherty PG, Pei DH. Monitoring the cytosolic entry of cell-penetrating peptides using a pH-sensitive fluorophore. Chem Commun 2015;51:2162–5.
11. Wu MY, Li K, Liu YH, Yu KK, Xie YM, Zhou XD, Yu XQ. Mitochondria-targeted ratiometric fluorescent probe for real time monitoring of pH in living cells. Biomaterials 2015;53:669–78.
12. Liu Z, Peng CN, Guo CX, Zhao YY, Yang XF, Pei MS, Zhang GY. Novel fluorescent and colorimetric pH sensors derived from benzimidazo [2,1-a]benz[de]isoquinoline-7-one-12-carboxylic acid. Tetrahedron 2015;71:2736–42.
13. Saha UC, Dhara K, Chattopadhyay B, Mandal SK, Mondal S, Sen S, Mukherjee M, Smaalen SV, Chattopadhyay P. A new half-condensed Schiff base compound: highly selective and sensitive pH-responsive fluorescent sensor. Org Lett 2011;13:4510–3.
14. Gui RJ, An XQ, Huang WX. An improved method for ratiometric fluorescence detection of pH and Cd^{2+} using fluorescein isothiocyanate-quantum dots conjugates. Anal Chim Acta 2013;767:134–40.
15. McMahon BK, Pal R, Parker D. A bright and responsive europium probe for determination of pH change within the endoplasmic reticulum of living cells. Chem Commun 2013;49:5363–9.
16. Liu MJ, Ye ZQ, Xin CL, Yuan JL. Development of a ratiometric time-resolved luminescence sensor for pH based on lanthanide complexes. Anal Chim Acta 2013;761:149–56.
17. Lv HS, Huang SY, Zhao BX, Miao JY. A new rhodamine B-based lysosomal pH fluorescent indicator. Anal Chim Acta 2013;788:177–82.
18. Zhao XX, Chen XP, Shen SL, Li DP, Zhou S, Zhou ZQ, Xiao YH, Xi G, Miao JY, Zhao BX. A novel pH probe based on a rhodamine–rhodamine platform. RSC Adv 2014;4:50318–24.
19. Tan YQ, Yu JC, Gao JK, Cui YJ, Wang ZY, Yang Y, Qian GD. A fluorescent pH chemosensor for strongly acidic conditions based on the intramolecular charge transfer (ICT) effect. RSC Adv 2013;3:4872–5.
20. Yang MY, Song YQ, Zhang M, Lin SX, Hao ZY, Liang Y, Zhang DM, Chen PR. Converting a solvatochromic fluorophore into a protein-based pH indicator for extreme acidity. Angew Chem Int Ed 2012;51:7674–9.
21. Best QA, Liu CJ, van Hoveln PD, McCarroll ME, Scott CN. Anilinomethylrhodamines: pH sensitive probes with tunable photophysical properties by substituent effect. J Org Chem 2013;78:10134–43.
22. Yuan L, Lin WY, Chen B, Xie YN. Development of FRET-based ratiometric fluorescent Cu^{2+} chemodosimeters and the applications for living cell imaging. Org Lett 2012;14:432–5.
23. Yang Z, She MY, Yin B, Cui JH, Zhang YZ, Sun W, Li JL, Shi Z. Three rhodamine-based 'off-on' chemosensors with high selectivity and sensitivity for Fe^{3+} imaging in living cells. J Org Chem 2012;77:1143–7.
24. Bhalla V, Roopa KM, Sharma PR, Kaur T. New fluorogenic sensors for Hg^{2+} ions: through-bond energy transfer from pentaquinone to rhodamine. Inorg Chem 2012;51:2150–6.
25. Hasegawa T, Kondo Y, Koizumi Y, Sugiyama T, Takeda A, Ito S, Hamada F. A highly sensitive probe detecting low pH area of HeLa cells based on rhodamine B modified beta-cyclodextrins. Bioorg Med Chem Lett 2007;17:6015–9.
26. Zhu H, Fan JL, Xu QL, Li HL, Wang JY, Gao P, Peng XJ. Imaging of lysosomal pH changes with a fluorescent sensor containing a novel lysosome-locating group. Chem Commun 2012;48:11766–8.
27. Kang S, Kim S, Yang YK, Bae S, Tae J. Fluorescent and colorimetric detection of acid vapors by using solid-supported rhodamine hydrazides. Tetrahedron Lett 2009;50:2010–2.

28. Best QA, Xu RS, McCarroll ME, Wang LC, Dyer DJ. Design and investigation of a series of rhodamine-based fluorescent probes for optical measurements of pH. Org Lett 2010;12:3219–21.
29. Liu CJ, Best QA, Suarez BB, Pertile J, McCarroll ME, Scott CN. Cycloalkylaminomethyl rhodamines: pH dependent photophysical properties tuned by cycloalkane ring size. J Fluoresc 2015;25:231–7.
30. Zhang X, Jing XY, Huang SY, Zhou XY, Bai JM, Zhao BX. New fluorescent pH probes for acid conditions. Sensor Actuat B Chem 2015;206:663–70.
31. Liu LJ, Guo P, Chai L, Shi Q, Xu BH, Yuan JP, Wang XG, Shi XF, Zhang WQ. Fluorescent and colorimetric detection of pH by a rhodamine-based probe. Sensor Actuat B Chem 2014;194:498–502.
32. Xu Y, Jiang Z, Xiao Y, Bi FZ, Miao JY, Zhao BX. A new fluorescent pH probe for extremely acidic conditions. Anal Chim Acta 2014;829:146–51.
33. Ma QJ, Li HP, Yang F, Zhang J, Wu XF, Bai Y, Li XF. A fluorescent sensor for low pH values based on a covalently immobilized rhodamine–naphthalimide conjugate. Sensor Actuat B Chem 2012;68:166–7.
34. Tan JL, Zhang MX, Zhang F, Yang TT, Liu Y, Li ZB, Zuo H. A novel 'off-on' colorimetric and fluorescent rhodamine-based pH chemosensor for extreme acidity. Spectrochim Acta A Mol Biomol Spectrosc 2015;140:489–94.
35. Ge F, Ye H, Luo JZ, Wang S, Sun YJ, Zhao BX, Miao JY. A new fluorescent and colorimetric chemosensor for Cu(II) based on rhodamine hydrazone and ferrocene unit. Sensor Actuat B Chem 2013;181:215–20.
36. Zhang XF, Zhang T, Shen SL, Miao JY, Zhao BX. A ratiometric lysosomal pH probe based on the naphthalimide-rhodamine system. J Mater Chem B 2015;3:3260–6.
37. Shen SL, Zhang XF, Bai SY, Miao JY, Zhao BX. A novel ratiometric pH probe for extreme acidity based on FRET and PET. RSC Adv 2015;5:13341–6.
38. Shen SL, Chen XP, Zhang XF, Miao JY, Zhao BX. A rhodamine B-based lysosomal pH probe. J Mater Chem B 2015;3:919–25.
39. Zhang XF, Zhang T, Shen SL, Miao JY, Zhao BX. A ratiometric lysosomal pH probe based on the coumarin–rhodamine FRET system. RSC Adv 2015;5:49115–21.

Supporting information

Additional supporting information may be found in the online version of this article at the publisher's web site.